Pulsating Red Giants in a Globular Cluster: 47 Tucanae

John R. Percy
Prateek Gupta
Department of Astronomy and Astrophysics, and Dunlap Institute for Astronomy and Astrophysics, University of Toronto, 50 St. George Street, Toronto, ON M5S 3H4, Canada; john.percy@utoronto.ca

Received August 19, 2021; revised September 13, 2021; accepted September 22, 2021

Abstract We have carried out time-series analysis of a sample of 12 pulsating red giants (PRGs) in the globular cluster 47 Tuc, using observations from the ASAS-SN database, and the AAVSO software package VStar. Most (11/12) of the stars were classified by ASAS-SN as semiregular (SR). We have determined pulsation periods (P) for all 12 of them, and "long secondary periods" (LSPs) for 11 of them. This confirms that LSPs are common in Population II stars. In the context of recent explanations for LSPs, our results imply that many Population II red giants have accreting planetary companions, surrounded by dust. In over half the stars, the period given in the ASAS-SN catalogue is actually the LSP, not the pulsation period. About half the stars show some evidence of a second pulsation period, presumably a second pulsation mode. The amplitudes of the pulsation periods vary by up to a factor of 3.4, on time scales of 10 to 35 pulsation periods (median value 18). The average ratio of LSP to P is 9.0, but the values cluster around 5 and 10. This suggests that some of the stars are pulsating in a lower-order mode, but most are pulsating in a higher-order mode, and half are pulsating in both. The complex variability of the stars in our sample is similar to that of nearby PRGs with a solar composition. The fact that there are about 150 Galactic globular clusters, each with potentially-variable red giants, means that there are many opportunities for studies, like ours, by students and by amateur astronomers with an interest in data analysis, as well as by professional astronomers.

1. Introduction

Globular clusters (GCs), each with hundreds of thousands of stars, are among the oldest objects in our Milky Way (MW) galaxy, ten billion years old, or more. There is a halo of about 150 GCs around the MW. They are not just older than the Sun and most other stars, they also have a much lower abundance of elements heavier than helium—the so-called "metals." They are called "Population II stars."

The brightest stars in GCs are red giants, and red giants are unstable to radial pulsation. Red giant pulsation is complex. Stars can pulsate in one or more of several possible radial modes, and there are also "long secondary periods" (LSPs, Wood 2000). Their cause was unknown until recently (e.g. Takayama and Ita 2020), though the existence of an LSP-luminosity relation parallel to pulsation period-luminosity relations (Wood 2000) was an important clue. Both the pulsation periods and the pulsation amplitudes are variable on time scales of tens of pulsation periods.

In an important development, Soszyński *et al.* (2021) have made a very strong case that LSPs are due to binarity; they are due to the presence of a dusty cloud orbiting the red giant together with a low-mass companion, and obscuring the star once per orbit. The low-mass companion is a former planet which has accreted a significant amount of mass from the envelope of the red giant, and grown into a brown dwarf or low-mass star. The key evidence for this model is the presence of a secondary eclipse in the LSP cycle, seen in the mid-infrared, when the dusty cloud is behind the star.

We were curious to know whether Population II pulsating red giants (PRGs) showed the same complex variability as nearby, more metal-rich stars. This comparison might provide clues as to the cause of the complexities.

GCs have the advantage that the stars in them have very similar compositions, masses, ages, and distances. Variable stars have been studied in these clusters for over a century, but most of the attention has been devoted to RR Lyrae stars. These short-period (0.3 to 1.0 day) variables have well-defined luminosities, so they are a key "standard candle" in the cosmic distance scale. To study these variables, observers made closely-spaced observations for a few days. Clement (2021) maintains a very useful on-line catalogue of variable stars in globular clusters.

PRGs have periods of tens to hundreds of days, and were therefore not well-studied by short runs of closely-spaced observations. However, the All-Sky Automated Survey for Supernovae (ASAS-SN; Shappee *et al.* 2014, Kochanek *et al.* 2017) images the sky every day or two with a network of remote, robotic telescopes around the world. ASAS-SN has observed and catalogued half a million variables, all over the sky, and discovered many thousand new ones. Some of these are in GCs.

The ASAS-SN process for automated analysis, classification, and period determination of variables is not well-suited for the study of PRGs, and often produces incorrect or incomplete results (Percy and Fenaux 2019). In this paper, we do a detailed analysis or re-analysis of ASAS-SN observations of PRGs in one cluster.

We chose 47 Tuc, a bright, populous, well-studied cluster, about 13,000 LY (4 kpc) from the sun. We carefully examined the light curves to look for any of the possible complexities, and then used Fourier and wavelet analysis to study the periods, and changes in the pulsation amplitude. Our project extends the work of Lebzelter and Wood (2005), who obtained several hundred days of observations of several dozen red giants in 47 Tuc; see also Lebzelter *et al.* (2005). They identified many new variables, and determined periods for some known variables. However, their datasets were smaller and shorter than ours.

They determined periods, but not amplitudes (though these could be estimated from the light curves that they published), and did not estimate the values of the LSPs or look for multiperiodic behavior.

Our results are thus complementary to those of Lebzelter and Wood (2005) and of the ASAS-SN team, as well as other results in the literature as compiled by Clement (2021). The ASAS-SN datasets are longer than those of Lebzelter and Wood (2005), but not as long as the AAVSO visual datasets that are often used to study bright nearby PRGs.

Unfortunately ASAS-SN is not able to resolve stars in the dense cores of globular clusters, so it was not possible for us to study most of the stars in the Lebzelter and Wood (2005) sample. Our stars are in the halo of 47 Tuc, but are cluster members on the basis of their distances and proper motions.

This paper is also a "proof of concept" for similar studies of PRGs in GCs using the ASAS-SN database, which could include projects for students and for amateur astronomers with an interest in data analysis. There are many more clusters to be studied!

2. Data and analysis

We analyzed a sample of 12 stars (Table 1) from the ASAS-SN variable star catalogue (Shappee *et al.* 2014, Kochanek *et al.* 2017, Jayasinghe *et al.* 2018, 2019), in the GC 47 Tuc, within 30 arc minutes of the cluster center, and classified by ASAS-SN as Mira stars (visual range greater than 2.5 magnitudes), red semiregular (SR) variables, red irregular (L) variables, or "long secondary periods" (LSP). Almost all were SR. Lebzelter and Obbruger (2009) have shown that, for stars of similar physical properties, there is no essential difference in the pulsation properties of SR and L variables. The ASAS-SN data and light curves are freely available on-line (asas-sn.osu.edu/variables). The error bars on the ASAS-SN observations are 0.02 mag, and this is the noise level in our Fourier analyses.

In addition to very careful analysis of the visual light curve (e.g. Figure 1), we use the Fourier analysis and wavelet routines in the American Association of Variable Star Observers (AAVSO) time-series package VStar (Benn 2013). Note that the amplitudes which are given in this paper, including in the tables and figures, are actually semi-amplitudes—the coefficient of the sine curve with the given period—not the full amplitude or range.

Because of the complexity of the variability, and the different time scales involved, visual light curve analysis proved to be especially useful and important. The pulsational variability could be seen clearly, as could the LSP and the variability of the pulsational amplitude (Figures 1, 2, and 3). The intervals between maxima or minima could then be measured and averaged, yielding a period which was accurate to a few percent. Because of the variation of the pulsation amplitude, and the apparent mode switching in a few stars, it was also sometimes useful to inspect the light curve and do Fourier analysis of separate segments or seasons of the dataset.

Fourier analysis was used to confirm and refine the periods but, because of the low amplitudes, and the complexity of the variability, the peaks were often close to the noise level of 0.02 mag (Figure 4). However, the process of estimating the pulsation period(s) from the light curve made it clear which peak in the Fourier spectrum was the correct one. Once the pulsational period had been determined, wavelet analysis was used to study the range and time scale of the pulsational amplitude variability (Figure 5). The wavelet contour diagram was useful for detecting the presence of a second pulsation period and apparent mode-switching (Figure 6).

3. Results

Table 1 lists the ASAS-SN name, identifier (if any) in the Clement (2021) catalogue, type, period, V and K magnitudes, distance in kiloparsecs (from the ASAS-SN website), the primary pulsation period and LSP derived by us, and the ratio of the LSP to the pulsation period. The distance errors are typically 6 to 15 percent. Table 2 gives information about the pulsation amplitude variability—the maximum and minimum amplitudes, their ratio, and the approximate time scale of variability, in units of the pulsation period. This was determined by visual inspection of the amplitude-time graphs (e.g. Figure 5). Table 3 gives information about the stars with probable or possible bimodal behavior—the periods and their ratio. The three stars without an identifier in the Clement (2021) catalogue are presumably new discoveries.

The following are comments on individual stars, including previous periods, from Clement (2021), which appear to be approximations in most cases:

J002516.00-720355.0 This is a large-amplitude Mira star with a period of 193 days, and very little variation in pulsation amplitude. Previous period 192 days.

J002509.10-720215.3 A pulsation period of about 70 days is visible in the light curve (Figure 1), with strongly variable amplitude. There also appears to be an LSP of about 300 days, though the light curve is dominated by the pulsation and its variable amplitude. The Fourier analysis is somewhat uncertain; the LSP is 280 days, but there are pulsation periods of 70 and 78 days with comparable amplitudes. Wavelet analysis suggests that the most likely period is about 72.5 days. Previous period 80 days.

J002258.50-720656.3 A pulsation period of about 50 days and an LSP of about 240 days are visible in the light curve; these are refined to 53.9 and 244 days by Fourier analysis, though the signal is weak. There is also a pulsation period of about 38 days, which shows clearly in some segments of the light curve, and in the wavelet contour diagram. Previous period 40 days.

J002307.35-720029.8 A pulsation period of about 35 days and an LSP of about 380 days are visible in the light curve; these are refined to 35.3 and 377 days by Fourier analysis. There is also a period of 25.1 days which appears in the Fourier spectrum, and in some segments of the light curve.

J002503.68-720931.8 A pulsation period of about 45 days and an LSP of about 750 days are visible in the light curve; the variation in pulsation amplitude is clearly visible. The periods are refined to 45.5 and 769 days by Fourier analysis. Previous period 50 days.

J002355.01-715729.7 A pulsation period of about 40 days and an LSP of about 460 days are visible in the light curve.

Table 1. Period Analysis of ASAS-SN Observations of PRGs.

Name: ASAS-SN-V	*ID*	*Type*	*PA(d)*	*V*	*K*	*d(kpc)*	*P(d)*	*LSP(d)*	*LSP/P*
ASASSN-V J002516.00-720355.0	V3	M	194.4	11.65	6.31	4.834	193.2	—	—
ASASSN-V J002509.10-720215.3	V18	SR	233.3	11.83	6.63	3.626	72.5	280	3.9
ASASSN-V J002258.50-720656.3	V13	SR	255.3	11.54	7.66	4.017	53.9	244	4.5
ASASSN-V J002307.35-720029.8	—	SR	379.9	11.12	7.28	4.590	35.3	377	10.7
ASASSN-V J002503.68-720931.8	V5	SR	45.1	11.64	7.40	4.999	45.5	769	16.9
ASASSN-V J002355.01-715729.7	V17	SR	455.9	11.80	7.31	4.644	39.6	455	11.5
ASASSN-V J002217.84-720612.7	—	SR	37.7	11.75	7.60	4.070	37.7	225	6.0
ASASSN-V J002522.94-721105.1	V16	SR	30.0	11.49	7.23	4.363	30.1	328	10.9
ASASSN-V J002235.85-721110.9	V28	SR	443.2	11.91	6.89	4.066	51.4	444	8.6
ASASSN-V J002452.03-715611.0	LW20	SR	434.5	11.88	7.06	4.142	44.3	435	9.8
ASASSN-V J002422.81-715329.0	V10	SR	412.2	11.71	6.99	4.265	81.0	409	5.0
ASASSN-V J002330.09-722236.3	—	SR	59.3	12.11	6.79	3.886	60.3	701	11.6

Table 2. Amplitude Analysis of ASAS-SN Observations of PRGs.

Name: ASAS-SN-V	*Amax*	*Amin*	*Amax/ Amin*	*Time Scale/P*
ASASSN-V J002516.00-720355.0	1.39	1.31	1.1	8
ASASSN-V J002509.10-720215.3	0.12	0.04	3.4	14
ASASSN-V J002258.50-720656.3	0.07	0.03	2.4	18
ASASSN-V J002307.35-720029.8	0.03	0.01	3.0	29
ASASSN-V J002503.68-720931.8	0.18	0.08	2.2	27
ASASSN-V J002355.01-715729.7	0.05	0.03	1.6	16
ASASSN-V J002217.84-720612.7	0.08	0.03	2.5	18
ASASSN-V J002522.94-721105.1	0.04	0.02	2.0	33
ASASSN-V J002235.85-721110.9	0.14	0.05	2.9	31
ASASSN-V J002452.03-715611.0	0.10	0.03	3.3	21
ASASSN-V J002422.81-715329.0	0.05	0.03	1.6	12
ASASSN-V J002330.09-722236.3	0.20	0.08	2.5	10

Table 3. Analysis of ASAS-SN Observations of Bimodal PRGs.

Name: ASAS-SN-V	*Pb(d)*	*P(d)*	*Pb/P*
ASASSN-V J002258.50-720656.3	37.8	53.9	0.701
ASASSN-V J002307.35-720029.8	25.1	35.3	0.710
ASASSN-V J002355.01-715729.7	39.6	56.7	0.698
ASASSN-V J002522.94-721105.1	30.1	40	0.750
ASASSN-V J002452.03-715611.0	20.8:	44.3	0.470
ASASSN-V J002422.81-715329.0	41.3	81.4	0.510

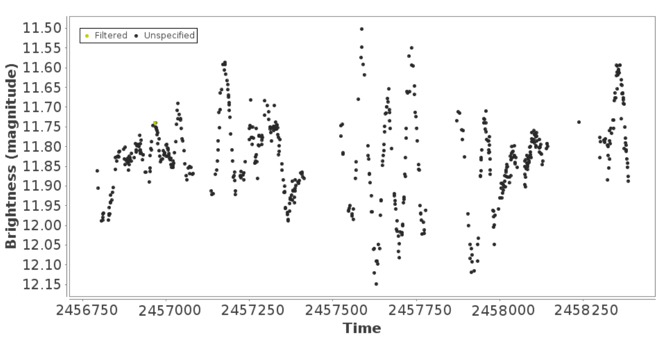

Figure 1. The V light curve of ASAS-SN-V J002509.10-720215.3. The pulsation period and the variability of its amplitude are clearly visible. The LSP is rather weak.

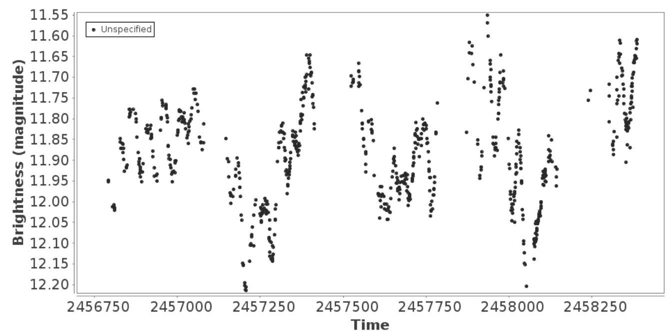

Figure 2. The V light curve of ASAS-SN-V J002452.03-715611.0. The pulsation period and the variability of its amplitude are clearly visible, as is the LSP.

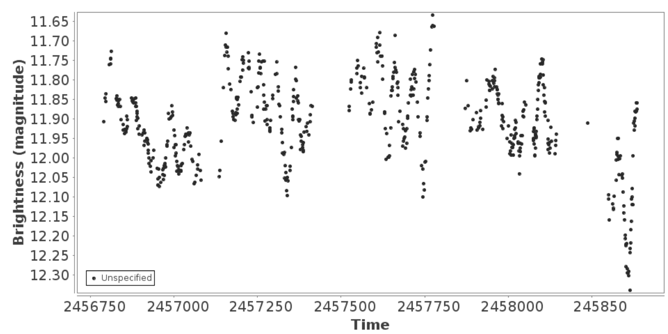

Figure 3. The V light curve of ASAS-SN-V J002235.85-721110.9. The pulsation period and the variability of its amplitude are clearly visible, as is the LSP.

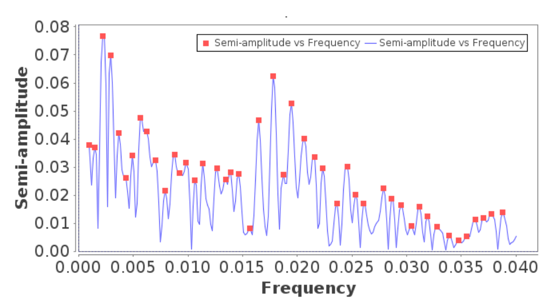

Figure 4. The Fourier spectrum of ASAS-SN-V J002235.85-721110.9, plotting semi-amplitude versus frequency in cycles per day. The pulsation period and LSP are clearly visible, along with their aliases. The light curve is shown in Figure 3.

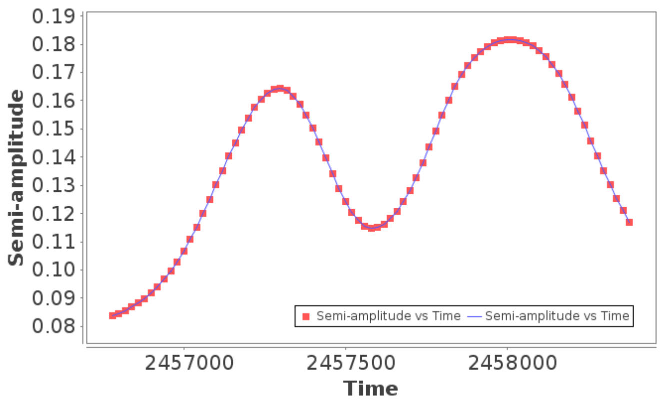

Figure 5. The variable pulsation semi-amplitude of ASAS-SN-V J002503.68-720931.8, as determined by wavelet analysis. The amplitude varies by a factor of two on a time scale of 800-1,000 days.

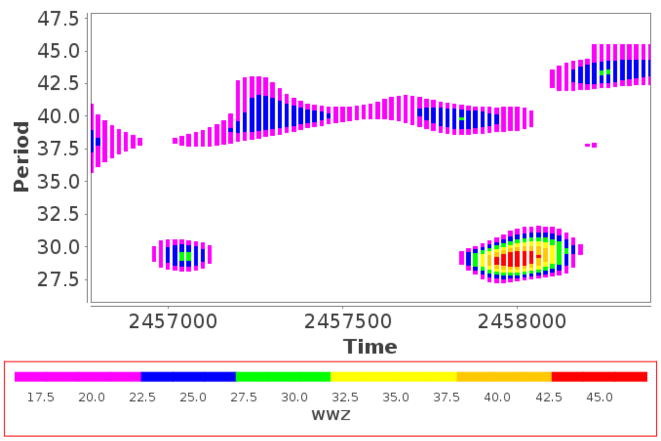

Figure 6. The wavelet contour diagram for ASAS-SN-V J002522.94-721105.1, plotting period in days versus Julian date, with WWZ amplitude in false color. It shows the presence of two pulsation modes with periods of about 30 and 40 days, each variable in amplitude, and apparent mode-switching on a time scale of about 1,000 days.

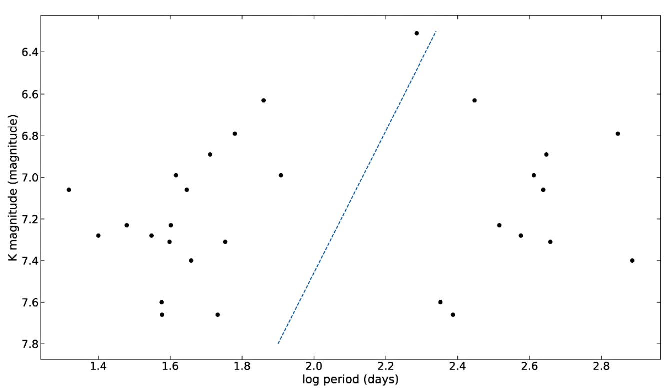

Figure 7. The period-luminosity relation (K magnitude versus log period) for all the periods of the 12 stars in our sample. The dashed line is sequence C (believed to represent the fundamental pulsation mode) for the stars studied by Lebzelter and Wood (2005). The points to the right of the line are LSPs; those to the left are pulsation periods, almost all pulsating in higher-order modes.

These periods are refined to 39.6 and 455 days by Fourier analysis. There is also a possible period of 56.7 days, which is also present in the wavelet contour diagram. Previous period 60 days.

J002217.84-720612.7 A pulsation period of about 35 days and an LSP of about 200–250 days are visible in the light curve, as is the variation in pulsation amplitude. The periods are refined to 37.7 and 225 days by Fourier analysis, though the signals are weak.

J002522.94-721105.1 A pulsation period of about 30 days and an LSP of about 330 days are visible in the light curve; these are refined to 30.1 and 328 days by Fourier analysis, though the amplitude is only 0.02 and the signals are close to the noise level. There is also evidence for a period of about 40 days in the Fourier and wavelet analysis (Figure 6). Previous period 41 days.

J002235.85-721110.9 A pulsation period of about 50 days, and an LSP of about 440 days are visible in the light curve, as is the variation in the pulsation amplitude (Figure 3). The periods are refined to 51.4 and 444 days by Fourier analysis (Figure 4). Previous period 40 days.

J002452.03-715611.0 A pulsation period of about 45 days, with variable amplitude, and an LSP of about 430 days are visible in the light curve. These are refined to 44.4 and 435 days by Fourier analysis. There is also some evidence for a second pulsation period of 20.8 days in the Fourier and wavelet analysis, but it is close to the noise level. There was one discrepant point in the light curve which was not used in the analysis. Previous period 49 days.

J002422.81-715329.0 A pulsation period of about 80 days, with variable amplitude, and an LSP of about 410 days are visible in the light curve. These are refined to 81.0 and 409 days by Fourier analysis. A possible pulsation period of 41.3 days is visible in the Fourier and wavelet analysis, but the amplitude is weak. Known variable, with no period given.

J002330.09-722236.3 A pulsation period of about 60 days and an LSP of about 700 days are clearly visible in the light curve. These periods are refined to 60.3 and 701 days by Fourier analysis. The amplitudes are relatively large.

4. Discussion

The pulsation periods of the 12 stars in Table 1 are a few tens of days, as expected. The stars in Table 3 show probable or possible bimodal behavior. Xiong and Deng (2007) have published pulsation models for red giants. They provide periods and period ratios for low-order radial pulsation modes. The stars in Table 3 with period ratios near 0.7 can be interpreted as pulsating in two adjacent modes. Those with ratios near 0.5 can be interpreted as pulsating in the fundamental and second, or first and third overtone.

LSPs are found in about a third of nearby field PRGs. In our sample, almost all the stars had LSPs. This may be because it is easier to detect them in small-amplitude pulsators, or because they are more common in Population II stars, or because ASAS-SN is more likely to have identified our stars as variable, and hence part of our sample. In any case, our results show that LSPs are very common in PRGs of both Population I and II. This is very interesting in the context of the Soszyński *et al.* (2021) model, since it shows that red giants with former planet companions, and dust clouds around them can exist in Population II stars. Furthermore, some of the binary orbits would be seen face-on, and would therefore not exhibit LSPs, so the incidence of binaries would be greater than the incidence of LSPs.

The ratios of LSP to P average 9.0, but cluster around 5 and 10. The same was found in bright field red giants by Percy and Leung (2017). Wood (2000) and subsequent workers who studied PRGs in stellar systems plotted period-luminosity sequences which they identified as LSP and low-order radial modes. Figure 7 shows such a diagram for our stars; those on the right are LSPs and those on the left are pulsation periods, and the dashed line is Lebzelter and Wood`s (2005) sequence for fundamental-mode pulsators. Our LSP/P ratios of 5 and 10 are consistent with the separations of these sequences. Specifically, they would correspond to the pulsation modes being primarily first or second overtone in our sample.

The pulsation amplitudes of the stars in our sample vary by up to a factor of 3.4 on a time scale of 10 to 35 pulsation periods (median value 18). In this respect, these Population II stars behave in the same way as nearby field stars (Percy and Abachi 2013). The cause of these variations is not known. For the bimodal variables, the pulsation amplitude variability can produce apparent "mode switching" which can be seen in the wavelet contour diagram (e.g. Figure 6). Note that the time scale for pulsation amplitude variation is a factor of two longer than the LSPs; there is no evidence that the two phenomena are related.

We note that only half of the pulsation periods that we have determined agree with the ASAS-SN period. In the other cases, the ASAS-SN period is the LSP. The ASAS-SN automated procedure chooses the best (i.e. the dominant) period, which may be either the pulsation period or the LSP. It does not allow for two or more periods.

The periods of these stars may also be variable, as is the case with bright nearby PRGs, whose periods "wander" in a way that can be modelled as random cycle-to-cycle fluctuations. We did not study possible period variability of this kind; our datasets are rather short for this.

This paper is based on a short (100 hours) summer research project by co-author PG, who had just completed the third year of an undergraduate astronomy and physics program. Projects of this kind are an excellent way for students to develop and integrate a wide range of skills in math, physics, and computing, motivated by the knowledge that they are doing real science, with real data. This paper is also an example of the type of project that could be done by skilled amateur astronomers with an interest in variable stars, data mining, and data analysis.

5. Conclusions

We have analyzed in detail the variability of 12 PRGs in the GC 47 Tuc, using ASAS-SN data. We derive pulsation periods for all 12, LSPs for 11, and possible second pulsation periods for 6 of them. The pulsation amplitudes vary by up to a factor of 3.4 on time scales of typically 20 pulsation periods. LSPs are common in these stars. The ratio of LSP to pulsation period averages 9.0, but the values cluster around 5 and 10. The ratio may reflect which mode the star is pulsating in. In all these respects, the PRGs in a metal-poor GC behave in the same way as nearby field variables with a solar composition.

6. Acknowledgements

This paper made use of ASAS-SN photometric data. We thank: the ASAS-SN project team for their remarkable contribution to stellar astronomy, and for making the data freely available on-line; the AAVSO for creating and making available the VSTAR time-series analysis package; and the anonymous referee for several suggestions which have improved this paper. We also acknowledge and thank the University of Toronto Work-Study Program for financial support. The Dunlap Institute is funded through an endowment established by the David Dunlap Family and the University of Toronto.

References

Benn, D. 2013, VSTAR data analysis software (https://www.aavso.org/vstar-overview).

Clement, C. M. 2021, "Catalogue of Variable Stars in Galactic Globular Clusters" (https://www.astro.utoronto.ca/~cclement/read.html).

Jayasinghe, T., *et al.* 2018, *Mon. Not. Roy. Astron. Soc.*, **477**, 3145.

Jayasinghe, T., *et al.* 2019, *Mon. Not. Roy. Astron. Soc.*, **486**, 1907.

Kochanek, C. S., *et al.* 2017, *Publ. Astron. Soc. Pacific*, **129**, 104502.

Lebzelter, T., and Obbruger, M. 2009, *Astron. Nachr.*, **330**, 390.

Lebzelter, T., and Wood, P. R. 2005, *Astron. Astrophys.*, **441**, 1117.

Lebzelter, T., Wood, P. R., Hinkle, K. H., Joyce, R. R., and Fekel, F. C.. 2005, *Astron. Astrophys.*, **432**, 207.

Percy, J. R., and Abachi, R. 2013, J. *Amer. Assoc. Var. Star Obs.*, **41**, 193.

Percy, J. R., and Fenaux, L. 2019, *J. Amer. Assoc. Var. Star Obs.*, **47**, 202.

Percy, J. R., and Leung, H. W.-H. 2017, *J. Amer. Assoc. Var. Star Obs.*, **45**, 30.

Shappee, B. J., *et al.* 2014, *Astrophys. J.*, **788**, 48.

Soszyński, I., *et al.* 2021, *Astrophys.J. Lett.*, **911**, L22.

Takayama, M., and Ita, Y. 2020, *Mon. Not. Roy. Astron. Soc.*, 492, 1348.

Wood, P. R. 2000, *Publ. Astron. Soc. Australia*, **17**, 18.

Xiong, D. R., and Deng, L. 2007, *Mon. Not. Roy. Astron. Soc.*, **378**, 1270.